ACS APPLIED MATERIALS & INTERFACES

Research Article

www.acsami.org

Solid Solution, Phase Separation, and Cathodoluminescence of GaP−ZnS Nanostructures

Baodan Liu,*[,†] Yoshio Bando,[‡] Benjamin Dierre,[§] Takashi Sekiguchi,[‡] Dmitri Golberg,[‡] and Xin Jiang*[,†]

[†]Shenyang National Laboratory for Materials Science, Institute of Metal Research (IMR), Chinese Academy of Sciences (CAS), No. 72 Wenhua Road, Shenyang 110016, China

[‡]World Premier International (WPI) Center for Materials Nanoarchitectonics (MANA), National Institute for Materials Science (NIMS), Namiki 1−1, Tsukuba, Ibaraki, 305-0044 Japan

[§]International Center for Young Center (ICYS)-MANA, National Institute for Materials Science (NIMS), 1-1 Namiki, Tsukuba, Ibaraki, 305-0044, Japan

Supporting Information

ABSTRACT: Quaternary solid-solution nanowires made of GaP and ZnS have been synthesized through well-designed synthetic routines. The as-synthesized GaP−ZnS solid-solution nanowires exhibit decent crystallinity with the GaP phase as the host, while a large amount of twin structural defects are observed in ZnS-rich nanowires. Cathodoluminescence studies showed that GaP-rich solid-solution nanowires have a strong visible emission centered at 600 nm and the ZnS-rich solid-solution nanowires exhibited a weak emission peak in the UV range and a broad band in the range 400−600 nm. The formation mechanism, processes, and optical emissions of GaP−ZnS solid-solution nanowires were discussed in detail.

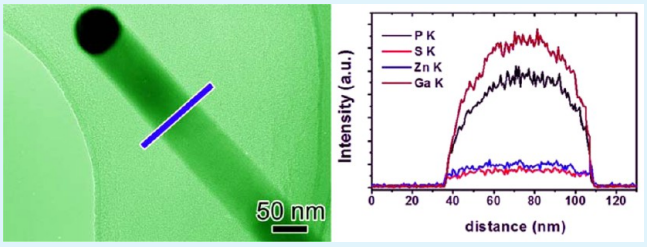

KEYWORDS: *solid solution, nanowires, synthesis, crystallography, optical property*

INTRODUCTION

Group III−V compounds, such as GaP or GaN crystals, have received considerable attention due to their technological applications in multi-color LEDs,[1,2] solar-fuel-cell conversion,[3] blue light emitters, and powerful high-temperature electronic devices.[4,5] As their peers, group II−VI compounds, like ZnO or ZnS, have also played key roles in the fields of various optoelectronic devices like LEDs, transistors,[6] diode lasers,[7] and photodetectors[8] in recent years. The combination of III−V and II−VI compounds will undoubtedly allow the formation of new structures with peculiar properties, and their properties can be artificially tailored through the composition controlling in the wide soluble range, if possible. However, their solidification in a wide composition range has demonstrated to be rather challenging and only few compound systems have been reported. The first example of a solid-solution structure made of III−V and II−VI compounds can be found in the GaAs−ZnSe system studied by Goryunova 50 years ago[9] and later was investigated in detail by Ku and Bodi.[10] The solid-solution system was further extended to a variety of pseudobinary compounds such as AlP−ZnS,[11] GaP−ZnS, or GaP−ZnSe reported by Yim[12] and Sonomura et al.[13] Recently, GaN−ZnO solid solutions in the form of nanoparticles and nanowires have been obtained through a solid-phase diffusion reaction at high temperature by Domen[14] and a template-conversion method by Han et al.[15] Such GaN−ZnO solid-solution nanostructures have been demonstrated to be an efficient and stable photocatalyst for hydrogen production through overall water splitting under visible light irradiation.[16] We have also synthesized the GaN−ZnO solid-solution nanowires with a zigzag morphology based on a vapor−liquid−solid (V−L−S) growth mechanism using Au nanoparticles as catalysts.[17] Using a similar method, well-crystallized GaP−ZnS solid-solution nanowires with a narrow solubility (<7 atm %) were also achieved, and their phase purity and crystallography have been systemically studied employing a high-resolution transmission electron microscope (TEM) equipped with an energy dispersive X-ray spectrometer (EDS).[17] Compared with the constituting compound, the solid-solution nanostructures have exhibited distinctive properties in optoelectronics and catalytic capability[14,17] and thus hold promising applications in a variety of fields.

In this paper, the crystallization process, phase separation, and growth mechanism of GaP−ZnS nanowires were systemically studied on the basis of detailed microstructural analysis using high-resolution TEM (HRTEM) and accurate composition characterization using the high-resolution EDS technique. The room-temperature cathodoluminescence (CL) properties of GaP−ZnS solid-solution nanowires with variable ZnS

Received: July 12, 2013
Accepted: August 27, 2013
Published: August 27, 2013

   dx.doi.org/10.1021/am4027949 | ACS Appl. Mater. Interfaces 2013, 5, 9199−9204

contents were also investigated, and their possible optical emission mechanism was discussed.

EXPERIMENTAL SECTION

The syntheses of GaP−ZnS solid-solution nanowires were carried out in a conventional horizontal electrical resistance furnace based on a V−L−S growth mechanism, in which Au nanoparticles were used as catalysts to promote the nanowire growth. A detailed experimental description of the synthetic routine for the formation of GaP−ZnS solid-solution nanostructures can be found in our previous published work.[17] It should be mentioned that the GaP and GaP-rich GaP−ZnS solid-solution (GaP being the main constituent) nanowires were grown on a Au-coated Si substrate, whereas the ZnS-rich GaP−ZnS solid-solution (ZnS being the main constituent) nanowires were synthesized on a Au-coated GaP substrate with the Ga and P atom incorporation into the ZnS lattice being directly from the surface decomposition of GaP substrate at high temperature. The morphology, phase purity, microstructures, and composition of as-grown nanowires were examined by means of a scanning electron microscope [(SEM) JEOL, JSM-6700F] and a high-resolution field-emission TEM [JEOL, JEM-3000F] equipped with an EDS system. The line-scan profiles in composition were recorded in a JEM-3100FEF field-emission transmission electron microscope (Omega Filter) in STEM mode. The CL spectra of GaP−ZnS nanowires were collected in a highly vacuumed field-emission SEM (Hitachi S4300) at an accelerated voltage of 5 kV and a beam current of 0.1 nA.[18]

RESULTS AND DISCUSSION

To form a solid-solution structure between two different compounds, it generally requires that the constituents should not only meet the structural matching, namely, the same structure and very close lattice constants that produce negligible lattice constrain to stabilize the mutually soluble structures, but also have a satisfied chemical compatibility which enables the heterovalent system energy preferentially. In addition, the used synthesis method and growth parameters also have an obvious effect on the solubility of solid-solution structure, as described in the GaP−ZnSe system and our previous study.[12,13,17] For GaP and ZnS compounds, they have the same structures and very close lattice constants, and their solidification has been demonstrated feasible in bulky crystal through the solution growth method. Therefore, a similar mutual combination process between GaP and ZnS compounds to form one-dimensional nanowires should be logically and experimentally possible on the basis of a well-designed synthesis routine and the careful controlling of growth parameters. Figure 1 shows the typical morphologies of GaP- and ZnS-rich GaP−ZnS solid-solution nanowires, respectively. One can see that the product with GaP as the host (the ratio of ZnS precursor in the initial powder source is less than 10 atm %) is comprised of a large yield of straight nanowires, which have a smooth morphology surface and uniform diameters in the range 50−200 nm (Figure 1a). Clear observation shows that each nanowire is terminated with an Au nanoparticle and their diameter is strictly confined by the particle size, demonstrating that the GaP-rich solid-solution nanowires are nucleated and crystallized under the assistance of Au catalyst particles. Figure 1b shows the morphology of ZnS-rich solid-solution nanostructures grown on a GaP substrate. Different from the GaP-rich GaP−ZnS nanowires, ZnS-rich nanostructures are composed of predominant solid-solution nanowires with rough morphology surface and a small fraction of impurity nanorods/nanoparticles. Unlike the GaP-rich nanowires with obvious catalyst particles, no catalyst particle is found on the tip

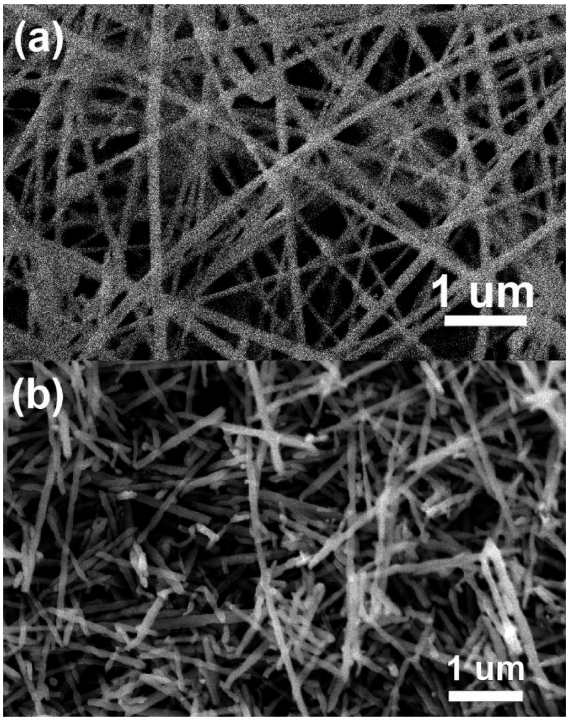

Figure 1. SEM images of (a) GaP-rich and (b) ZnS-rich GaP−ZnS solid-solution nanostructures.

end of ZnS-rich nanowires, possibly due to a quite different growth process.

Due to the different synthesis routines, the phase purity and solidification processes of GaP−ZnS solid-solution nanowires may be strongly influenced by the different ZnS ratios. Without ZnS incorporation, pure GaP nanowires are well-crystallized and free of any structural defect.[19] Increase of the ZnS ratio in the initial precursors up to a maximum content of 10 atm % can still stabilize the wire-like nanostructures. As an example, Figure 2a and b shows the low-magnification TEM images of GaP-rich GaP−ZnS solid-solution nanostructures. Typically, the nanowires with smooth morphology surface has a diameter range of 50−200 nm and some nanowires prefer to assemble together to form nanowire bundles (Figure 2b). Figure 2c shows a representative GaP−ZnS nanowire terminated with an Au particle, and one can see that the nanowire diameter is precisely guided by the Au nanoparticle size, demonstrating the catalytic function of Au nanoparticle and the V−L−S process involved in the nanowire formation.[20] The line-scan profiles using EDS along the radial direction of the nanowire, as schematically described in Figure 2c, demonstrated that the GaP and ZnS phases are completely and mutually mixed, as evidenced by the synchronous intensity changes of Ga, P, Zn, and S elements (Figure 2d). The relatively higher intensities of Ga and P signals compared with these of Zn and S elements conclude that the nanowires are GaP-dominant. The content of the ZnS phase in the GaP lattice can be roughly estimated to be ∼7 atm % through the quantitative analyses on tens of nanowires. Similarly, ZnS-rich GaP−ZnS solid-solution nanowires can also be obtained through an alternative method. Different from the catalytic formation of GaP-rich nanowires, ZnS-rich solid-solution nanowires were achieved through an in situ doping process during the crystallization of the ZnS phase at high temperature (∼1150 °C), in which the Ga and P atoms decomposed from the GaP substrate are simultaneously

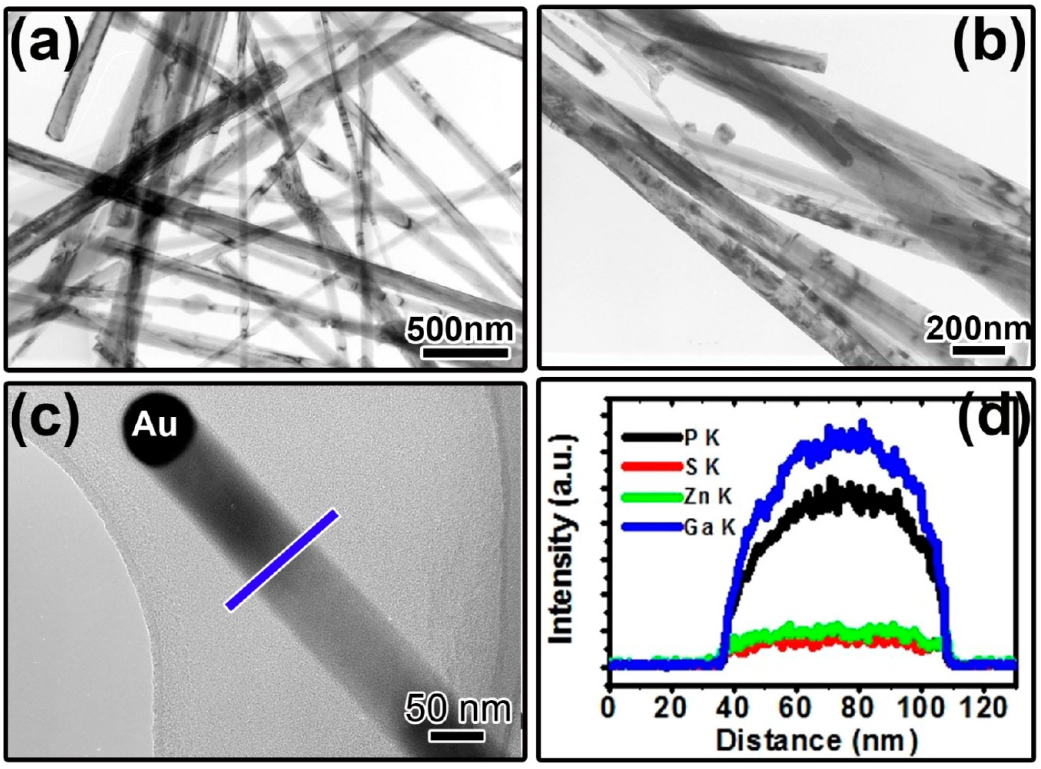

Figure 2. (a, b) Low-magnification TEM images of GaP-rich GaP−ZnS solid-solution nanowires; (c) representative GaP−ZnS solid-solution nanowire terminated with a Au nanoparticle; (d) X-ray dispersive line profiles of the constituting elemental Ga, P, Zn, and S intensities.

incorporated into the ZnS lattice, as schematically described in Figure S1 (Supporting Information). The spatial distributions of Ga and P atoms in the ZnS host are quite uniform and can be verified through the line-scan curves (Figure S1, Supporting Information). The maximum content of GaP in the ZnS lattice can be estimated to be ∼5 atm % using the same quantitative analysis in EDS measurement.

In fact, extensive efforts have been made to obtain GaP−ZnS solid-solution nanowires with continuous ZnS compositions by tuning the ratios of GaP and ZnS powders in initial precursors. Unfortunately, further increase of the ZnS content excessive to 10 atm % in the initial precursors will lead to an obvious morphology evolution and the wire-like morphology will evolve to necklace-like nanostructures, as shown in Figure 3a. Typically, the necklace-like structure is composed of some beads with a uniform diameter of 400 nm (Figure 3c) and a thin nanowire linking all these nanobeads together (Figure 3a). The diameter of the nanowire is around 50 nm and contains a large amount of twin defects, reflected by the obvious contrast in brightness (Figure 3b). The structural analyses on the bead and the central nanowire using high-resolution TEM concluded that the bead is amorphous, whereas the nanowire is crystalline but containing periodic twin defects along the axial direction. The HRTEM image and corresponding selected area electron diffraction (SAED) pattern can well verify the amorphous characteristic of the bead (Figure 3d). Similarly, the HRTEM analysis performed on the edge of the nanowire showed that a large number of twins exist along the ⟨111⟩ direction and the atomic layers to form the twin are not fixed, as shown in Figure 3e. Further analysis using SAED pointed out that the twin is composed of two (220) planes mirrored by the (111) boundary (Figure 3f). The X-ray line-scan measurement performed along the radial direction of the nanowire (shown in Figure 2b) demonstrated that an obvious phase separation has occurred due to the adding of excessive ZnS powders in initial precursors (Figure 3g). From the line-scan profiles, we can further confirm that the nanowire actually exhibits a core-shell structure with a 19 nm GaP phase as the core and a ZnS shell thickness of 11 nm. The necklace-like morphology of GaP−ZnS nanostructures can be well maintained in a wide range of ZnS content up to 75 atm % in initial precursors. Further increase of the ZnS content will result in the expansion of the beads along the nanowire direction and make them linking together (Figure S2, Supporting Information). From series of growth experiments, it has been found that the phase purity of GaP−ZnS nanostructures is extremely sensitive to the growth parameters such as reaction temperature, precursor ratios, gas flowing rate, etc., and wire-like GaP−ZnS core-shell nanostructures have also been synthesized using a similar method.[21]

For the syntheses of all GaP−ZnS solid-solution nanowires, Au nanoparticles are used to assist the nanowire growth due to their extremely superior catalytic function. Figure 4a depicts the formation process of GaP−ZnS nanowires with Au nanocatalyst involved. Typically, Au nanoparticles will first melt into some liquid droplets with an active surface at a high temperature; when the constituent atoms (Ga, P, Zn, and S) decomposed from initial GaP and ZnS powders are transported into the substrate position in the form of vapor or liquid, they will be absorbed on the Au droplet surface and be dissolved into it; with the continuous supplying of precursor atoms, the four constituent elements will become saturated in Au droplet and separate out to form a quarternary solid-solution nanocrystal. It should be noted that the formation of ZnS-rich solid-solution nanowires may nucleate and crystallize in a different process in which the deposited Au layer does not act as a catalyst, since no catalyst particle was found on the

dx.doi.org/10.1021/am4027949 | ACS Appl. Mater. Interfaces 2013, 5, 9199−9204

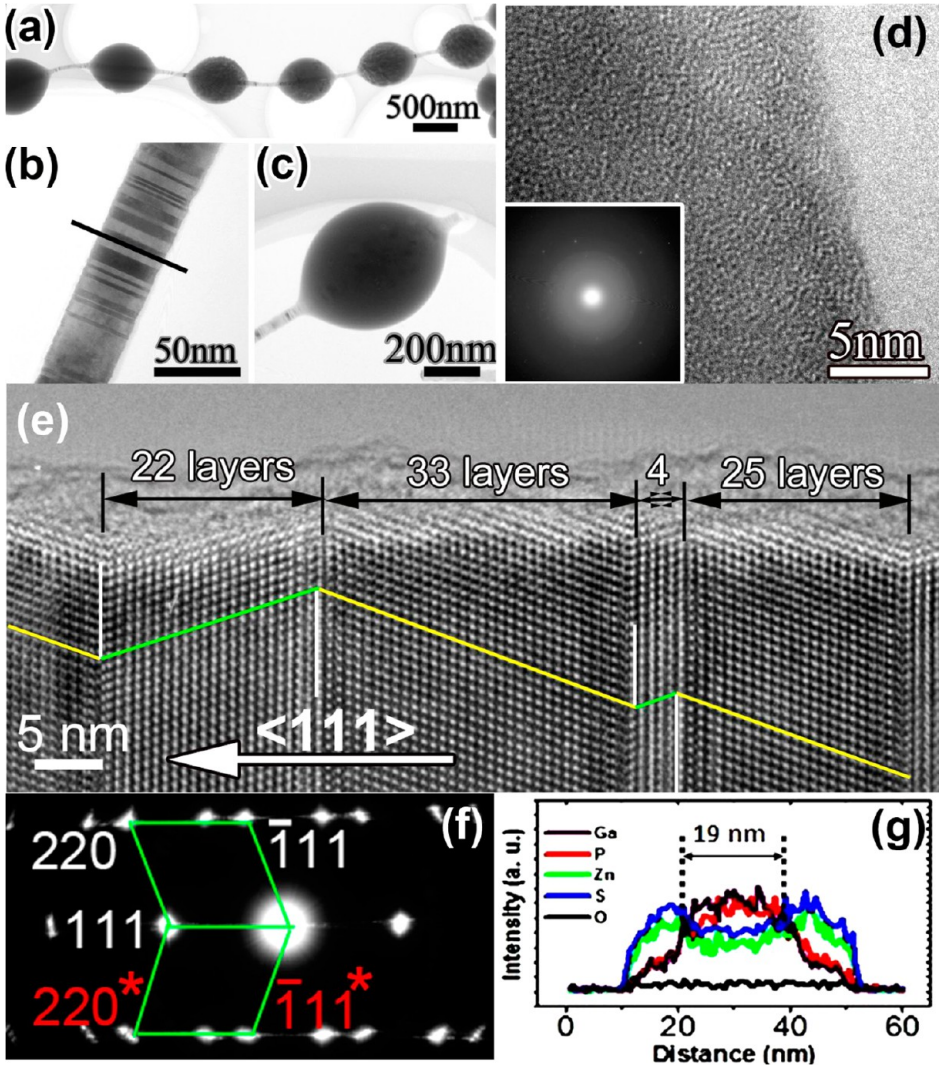

Figure 3. (a) Low-magnification TEM image of a necklace-like GaP−ZnS nanostructure; (b, c) TEM images of the central nanowire and bead; (d) HRTEM image of the bead shown in part c (the inset is the corresponding SAED pattern); (e) HRTEM image of the central nanowire shown in part b; (f) the corresponding SAED pattern of part e; (g) X-ray line-scan profiles of Ga, P, Zn, S, and O elements as schematically performed in part b.

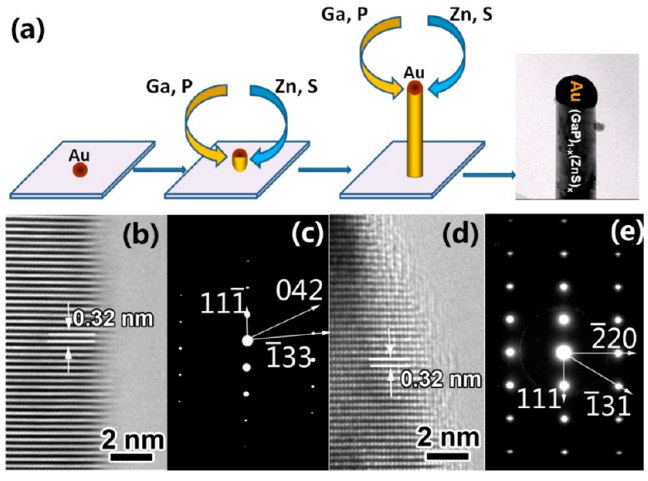

Figure 4. Schematic diagram of the GaP−ZnS solid-solution nanowire formation controlled by a Au nanocatalyst.

nanowire end. In order to examine the phase purity and crystal quality of as-synthesized GaP−ZnS solid-solution nanowires, high-resolution TEM and SAED analyses were carried out. Figure 4b−e shows the atomic images and their corresponding SAED patterns along different zone axes for an exampled nanowire with GaP as the dominant constituent. It can be seen that the GaP-rich solid-solution nanowires are highly crystallized, and all the atoms are regularly arranged in an fcc-type structure. The succinctness of the SAED patterns taken from different zone axes also proves the good crystallization of GaP−ZnS solid-solution nanowires. However, the defect-free crystallization cannot be found in ZnS-rich solid-solution nanowires and a large amount of twins with nonperiodic atomic layer thickness will be observed (Figure S3, Supporting Information). Appearance of the twins in ZnS-rich GaP−ZnS solid-solution nanowires is possibly related to the critical growth process, in which the P and Ga atoms escaping from the GaP substrate surface and incorporating into ZnS lattice require a rather stable temperature, whereas the actual temperature may slightly fluctuate to destroy the dynamic equilibrium. As a

result, the twin defects are finally formed in the ZnS-rich solid-solution nanowires.

Figure 5 shows the CL spectra of pure GaP nanowires and GaP-rich and ZnS-rich solid-solution nanowires under an

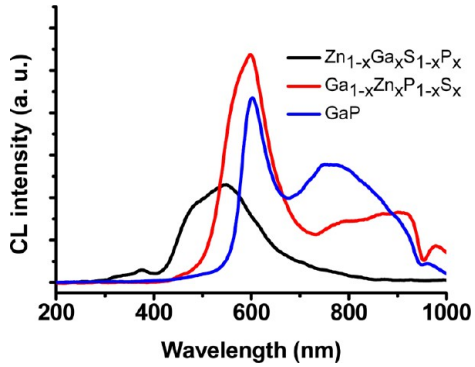

Figure 5. CL spectra of GaP and GaP−ZnS solid-solution nanowires.

applied voltage of 5 kV and a beam current of 0.1 nA. The GaP nanowires with a smooth surface exhibit a strong visible emission with a maximum peak wavelength centered at 600 nm and a broad shoulder in the range 700−1000 nm. This green emission has been observed in our previous GaP nanowires and nanoflowers[19] and can be regarded as the near-band-edge (NBE) emission of a zinc-blende-type GaP that originates from the effect of twin structural defects[22] or the inevitable impurity incorporation during nanowire nucleation.[23] The band-to-band transition was not observed in the current GaP nanowires. The broad emission in the range 700−1000 nm can be assigned to the donor−acceptor radiative recombination in the band, as observed in GaP nanowires and nanoflowers.[19] After solidification with ZnS (5 atm %), the maximum peak intensity of GaP−ZnS nanowires increases apparently and the nanowires become more luminescent. Furthermore, the green emission band also becomes broader: the maximum peak is at ∼600 nm, and an obvious shoulder in the range 500−600 nm is observed (Figure 5, red curve), which means that the incorporation of ZnS constituent into the GaP lattice leads to the obvious shift of the green band towards the UV wavelength direction. During the solidification process, the Zn and S atoms will randomly occupy the Ga and P sites, respectively, in a zinc-blende-type fcc structure. In fact, a similar luminescence phenomenon has also been reported in previously published work on GaP−ZnS solid-solution bulky film, in which the band-gap (or maximum peak position) of GaP-rich GaP−ZnS crystal was almost independent on the ZnS content increase in the range 0−30 atm %.[13] It is believed that the solidification process in the GaP−ZnS system is quite complex. A reasonable interpretation for the band-gap independence on ZnS content in GaP-rich solid-solution nanowires may come from the fact that the photon transition process in GaP−ZnS nanowires is actually governed by the unconfirmed deep recombination centers, and thus, the monotonic peak shift towards the UV direction is not observed in either the nanostructured or bulky GaP−ZnS system. Compared with the strong luminescence intensity of pure GaP nanowires in the wavelength range 700−1000 nm, the CL spectrum of GaP-rich solid-solution nanowires only shows a small tail and the peak intensity has decreased sharply, indicating that the donor−acceptor recombination process in the GaP lattice has been greatly weakened due to the substitutions of anions (S) and cations (Zn). With further increase of the ZnS content, the ZnS-rich solid-solution nanowires exhibit extremely different optical emissions. The band in the 700−1000 nm range disappears and a new broad emission band with a peak wavelength of 545 nm in the range 400−600 nm is formed. This band can be assigned to the defect-related emission caused by the formation of twin defects in ZnS−GaP nanowires (the incorporation of GaP in the ZnS lattice has resulted in numerous twin defects, as presented in Figure S3, Supporting Information), and a similar CL emission peak centered in the range 380−550 nm has been observed in T-shaped ZnS nanostructures that contain twinned defects.[24] It should be noted that the slight shift of the emission peak due to the introduction of GaP in the ZnS lattice is possible and the adding of Ga and P atoms may partially change the band structure of ZnS. It has been reported that the band of the GaN crystal can be tailored through the p−d repulsion of N_{2p} and Zn_{3d} orbitals after alloying with ZnO.[14] Additionally, we can also observe a small band with lower intensity and a maximum peak centered at 375 nm in ZnS-rich solid-solution nanowires. This emission should be related to the NBE transition of a zinc-blende-type ZnS. Similar to the band expansion in the ZnS doped GaP lattice matrix, the GaP incorporation into the ZnS lattice matrix may also induce the band shrinking and this has been confirmed in the bulky GaP−ZnS system.[12] Though the exact intrinsic band-gap of ZnS−GaP solid solution with a 5 atm % GaP dopant is not known, the 375 nm emission should not originate from its band-to-band transition due to the existence of a large amount of twin structural defects.

From the above results, we can see that the solidification process in a pseudobinary semiconductor system is rather complex and it requires harsh prerequisitions in the matching of crystal structure and chemical compatibility, as well as a good control of nucleation process. Especially, the composition homogeneity in a nanoscaled structure becomes more challenging and a slight vibration of the growth parameters (temperature and precursor flux, etc.) from the ideal equilibrium state will strongly affect the uniformity in crystallinity, composition, and size of nanostructures; thus, some unexpected properties in optics and electronics will be presented. For example, the resistivity of GaP structure is extremely sensitive to the adding of ZnS[17] and a slight incorporation of ZnS in GaP lattice matrix will lead to the exponential increase of resistivity.[13] Therefore, the solid-solution nanostructures made of pseudobinary or multi-component semiconductors may exhibit more intriguing properties and represent key members in the nanomaterial family.

CONCLUSIONS

In summary, GaP−ZnS solid-solution nanowires with narrow solubility have been synthesized through carefully designed chemical vapor deposition (CVD) processes. Incorporation of ZnS does not lead to the crystallinity deterioration of GaP nanowires in the soluble range, but the incorporation of GaP into the ZnS lattice matrix indeed causes the formation of twin structure defects in turn. Further increase of the ZnS ratio in initial precursors will lead to the phase separation and the formation of a necklace-like core-shell nanostructures. Correspondingly, the GaP-rich solid-solution nanowires exhibit a similar spectrum profile with that of pure GaP nanowires though a slight band shift towards the UV direction is observed, whereas the ZnS-rich nanowires show a broad emission band in the range 400−600 nm and a shoulder in the range 360−390

nm, distinctly different from that of GaP-rich nanowires. It is believed that the optical emission processes and mechanism in pseudobinary solid-solution semiconductor nanostructures are quite complex and may bring intriguing phenomena and technologically important applications in diverse fields if their growth and properties can be optimized and selectively controlled.

■ ASSOCIATED CONTENT

Supporting Information

Schematic diagram of the formation of ZnS-rich GaP−ZnS solid-solution nanowires, SEM image of necklace-like GaP−ZnS nanostructures, and HRTEM image of ZnS-rich GaP−ZnS solid-solution nanowires. This material is available free of charge via the Internet at http://pubs.acs.org.

■ AUTHOR INFORMATION

Corresponding Authors

*E-mail: baodanliu@imr.ac.cn.
*E-mail: xjiang@imr.ac.cn.

Notes

The authors declare no competing financial interest.

■ ACKNOWLEDGMENTS

B.L. thanks the Knowledge Innovation Program of Institute of Metal Research (Grant No. Y2NCA111A1) for the support of this work. B.D. is grateful to Tokodai Institute for Elemental Strategy (TIES) conducted by the Ministry of Education, Culture, Sports, Science and Technology (MEXT), Japan, for its funding.

■ REFERENCES

(1) Hwang, J. M.; Hung, W. H.; Hwang, H. L. *IEEE Photonics Technol. Lett.* **2008**, *20*, 608−610.
(2) Tatebayashi, J.; Mariani, G.; Lin, A.; Hicks, R. F.; Huffaker, D. L. *Appl. Phys. Lett.* **2010**, *96*, 253101-1−253101-3.
(3) Ohashi, K.; Mccann, J.; Bockris, J. O. M. *Nature* **1977**, *266*, 610−611.
(4) Chen, Q.; Khan, M. A.; Yang, J. W.; Sun, C. J.; Shur, M. S.; Park, H. *Appl. Phys. Lett.* **1996**, *69*, 794−796.
(5) Mohammad, S. N.; Morkoc, H. *Prog. Quantum Electron.* **1996**, *20*, 361−525.
(6) Hoffman, R. L.; Norris, B. J.; Wager, J. F. *Appl. Phys. Lett.* **2003**, *82*, 733−735.
(7) Wong, E. M.; Searson, P. C. *Appl. Phys. Lett.* **1999**, *74*, 2939−2941.
(8) Fang, X. S.; Bando, Y.; Liao, M. Y.; Gautam, U. K.; Zhi, C. Y.; Dierre, B.; Liu, B. D.; Zhai, T. Y.; Sekiguchi, T.; Koide, Y.; Golberg, D. *Adv. Mater.* **2009**, *21*, 2034−2039.
(9) Goryunova, N. A.; Fedorova, N. N. *Sov. Phys.-Solid State* **1959**, *1*, 307−308.
(10) Ku, S. M.; Bodi, L. J. *J. Phys. Chem. Solids* **1968**, *29*, 2077−2082.
(11) Addamiano, A. *J. Electrochem. Soc.* **1960**, *107*, 1006−1007.
(12) Yim, W. M. *J. Appl. Phys.* **1969**, *40*, 2617−2623.
(13) Sonomura, H.; Uragaki, T.; Miyauchi, T. *Jpn. J. Appl. Phys.* **1973**, *12*, 968−973.
(14) Maeda, K.; Teramura, K.; Takata, T.; Hara, M.; Saito, N.; Toda, K.; Inoue, Y.; Kobayashi, H.; Domen, K. *J. Phys. Chem. B* **2005**, *109*, 20504−20510.
(15) Han, W. Q.; Liu, Z. X.; Yu, H. G. *Appl. Phys. Lett.* **2010**, *96*, 183112-1−183112-3.
(16) Maeda, K.; Teramura, K.; Saito, N.; Inoue, Y.; Domen, K. *J. Catal.* **2006**, *243*, 303−308.
(17) Liu, B. D.; Bando, Y.; Liu, L. Z.; Zhao, J. J.; Masanori, M.; Jiang, X.; Golberg, D. *Nano Lett.* **2013**, *13*, 85−90.
(18) Liu, B. D.; Bando, Y.; Dierre, B.; Sekiguchi, T.; Tang, C. C.; Mitome, M.; Wu, A. M.; Jiang, X.; Golberg, D. *Nanotechnology* **2009**, *20*, 365705-1−365705-7.
(19) Liu, B. D.; Bando, Y.; Tang, C. C.; Golberg, D.; Xie, R. G.; Sekiguchi, T. *Appl. Phys. Lett.* **2005**, *86*, 083107−083107-3.
(20) Wagner, R. S.; Ellis, W. C. *Appl. Phys. Lett.* **1964**, *4*, 89−90.
(21) Hu, L.; Brewster, M. M.; Xu, X.; Tang, C.; Gradečak, S.; Fang, X. *Nano Lett.* **2013**, *13*, 1941−1947.
(22) Liu, B. Y.; Wei, L. W.; Ding, Q. M.; Yao, J. L. *Nanotechnology* **2004**, *15*, 1745−1748.
(23) Zhang, Z.; Senz, S.; Zhao, F. L.; Chen, L. J.; Gao, X. S.; Liu, J. M. *RSC Adv.* **2012**, *2*, 8631−8636.
(24) Liu, B. D.; Bando, Y.; Wang, Z. E.; Li, C. Y.; Gao, M.; Mitome, M.; Jiang, X.; Golberg, D. *Cryst. Growth Des.* **2010**, *10*, 4143−4147.